# A tunable nanocavity fiber laser based on hybrid halide perovskite nanocrystals

**Christos Grivas[1,2], Ming Ding[3,4], Pascal Harimech[2], Jean Schollhammer[1], Amin Baghban[1], Katia Gallo[1], Antonios G. Kanaras[2], Gilberto Brambilla[3]**

*[1]KTH–Royal Institute of Technology, Department of Applied Physics, Stockholm SE-106 91, Sweden*

*[2]School of Physics and Astronomy, University of Southampton, United Kingdom*

*[3]ORC, University of Southampton, Southampton SO17 1BJ, UK*

*[4] School of Instrumentation Science and Opto-electronics Engineering, Beihang University, Beijing 100191, PRC*

# Outline

1. Fabrication procedures (optical fiber tapers, tips, nanocavities)
2. Colloidal hybrid organic-inorganic and all-inorganic perovskite nanocrystals
3. Laser operation of hybrid nanocavities-wavelength tuneability
4. Quasi-cw lasing in 2D perovkite nanocrystals
5. Conclusions

# Fabrication Procedures

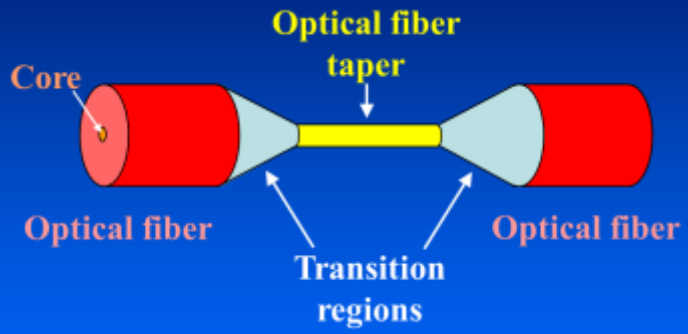


## flame brushing technique

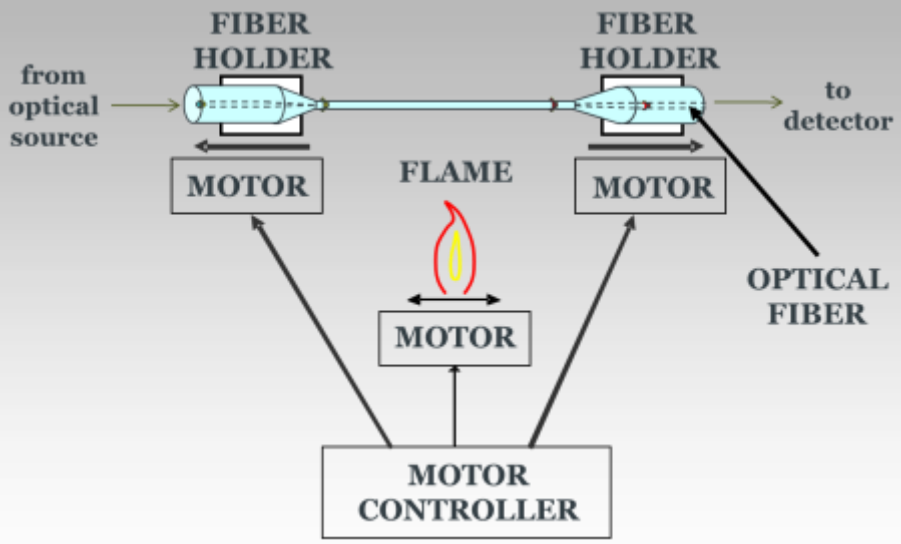


## MODIFIED
## flame brushing technique

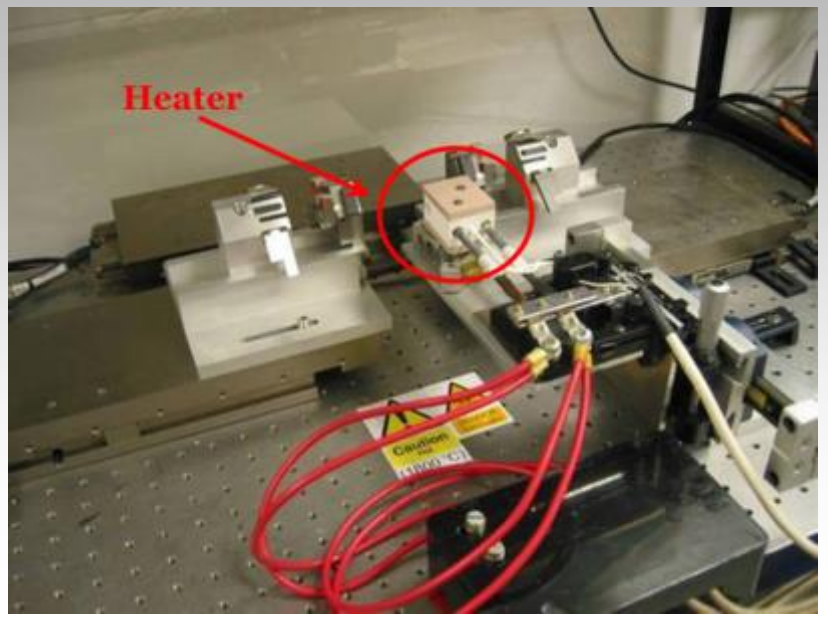

# Nanostructured tapered cavities

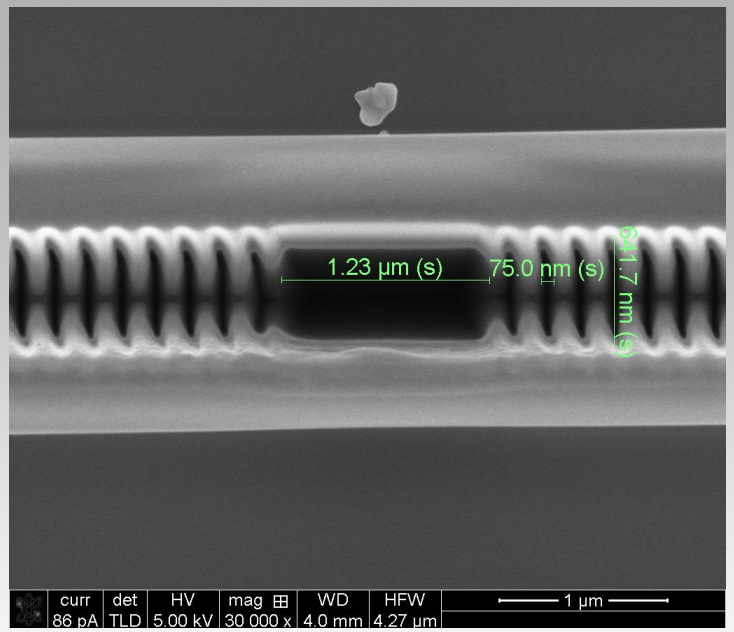


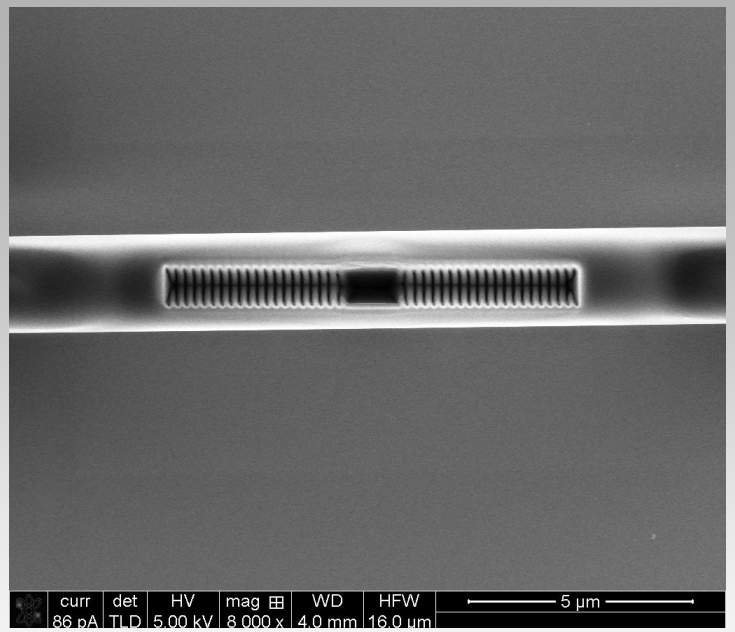


**Cavities patterned by focussed ion beam (FIB) milling* uniform waist length of the tapers**

* $Ga^+$ beam driven by an accelerating voltage of 30.0 kV and a current of 93 pA

# Hybrid perovskite semiconductor nanodots (I)

**General formula: $MPbX_3$, X=Cl, Br, I & M = $CH_3NH_3$**

- high gain coefficients and low amplification thresholds
- low defect densities and remarkable photostability
- tunability of their bandgap/emission wavelength across the visible spectrum, from ~390 to 790 nm by varying the ratio of halides in their composition.

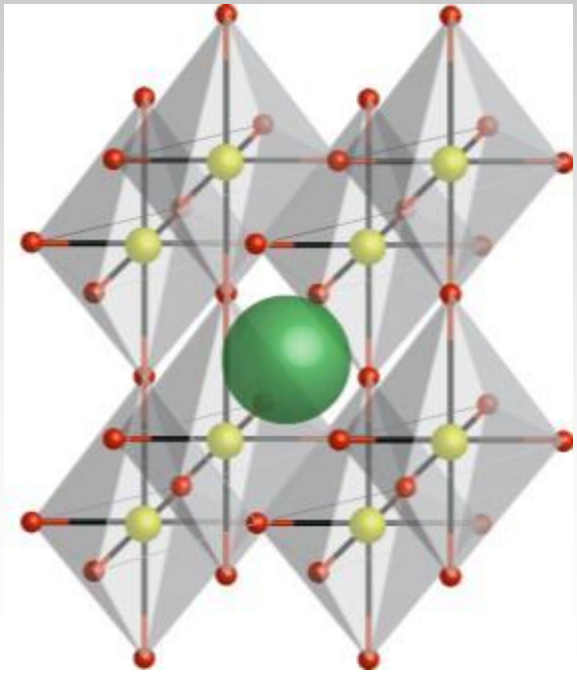

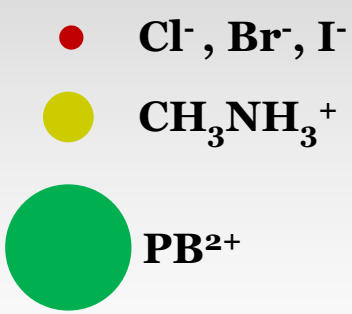


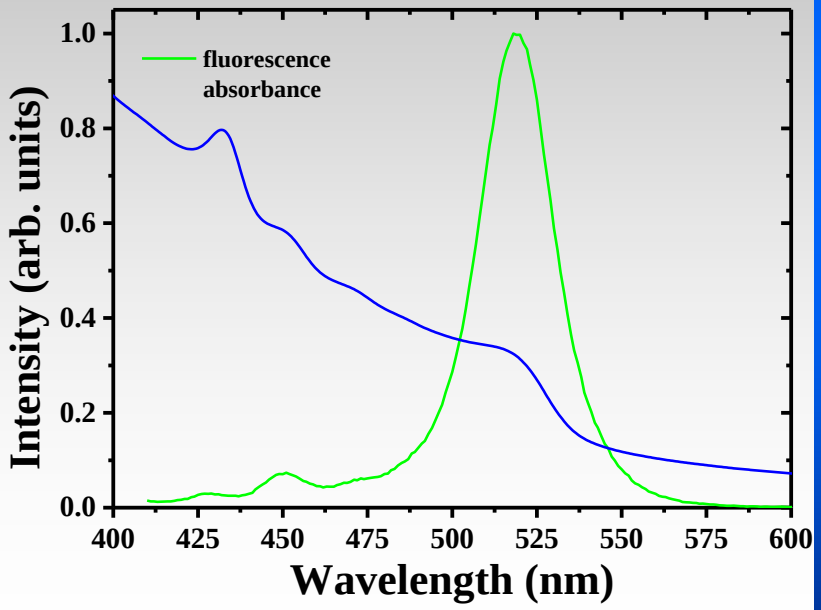

# Hybrid perovskite semiconductor nanodots (II)

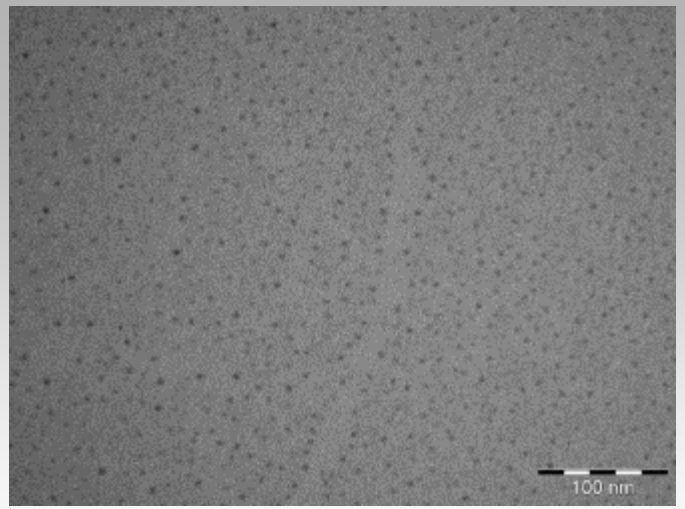


TEM micrographs of $MPbBr_3$ nanocrystals with spherical geometry

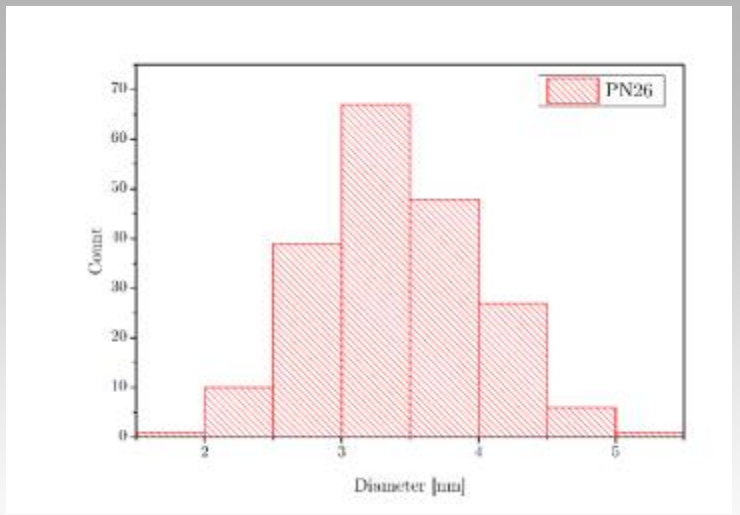


Size distribution of spherical $MPbBr_3$ nanocrystals

# Inorganic cesium lead halide perovskites

## General formula: $CsPbX_3$ (X = Br)

- high photoluminescence quantum yields reaching 90%
- low bimolecular recombination rates, slow Auger recombination
- Wavelength tuning from 410 to 700 nm by compositional control and to a certain extent by exploiting quantum-size effects.

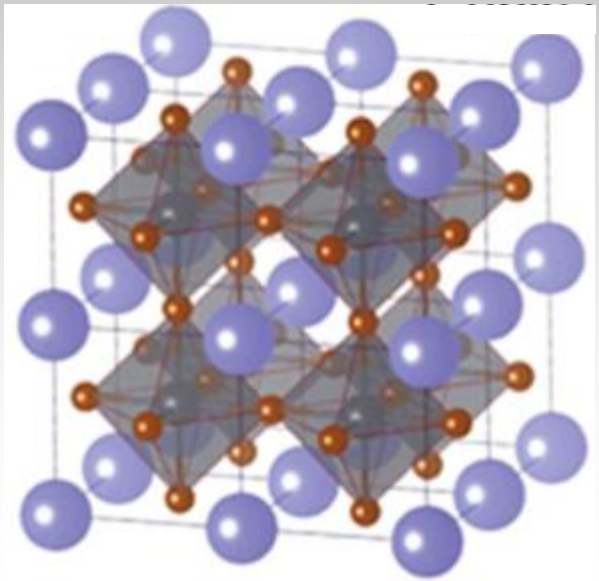

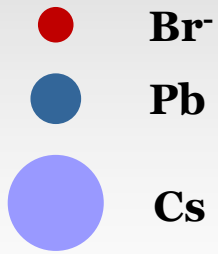


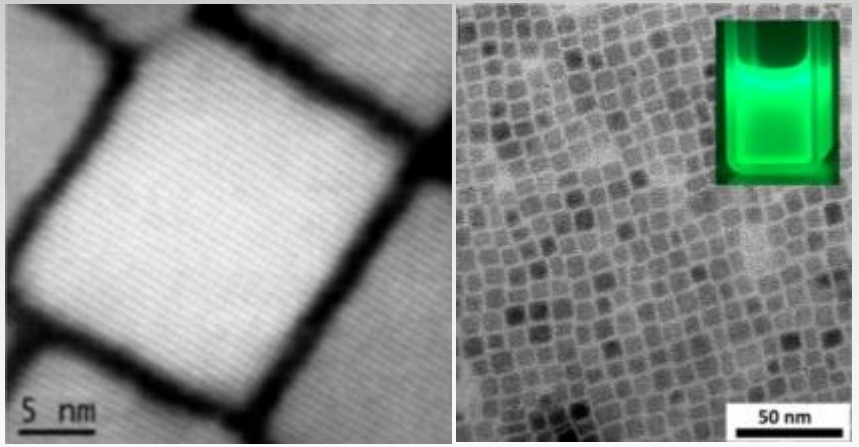


**TEM micrographs of green CsPbBr3 platelets**

# Nanolithographic deposition of perovskites

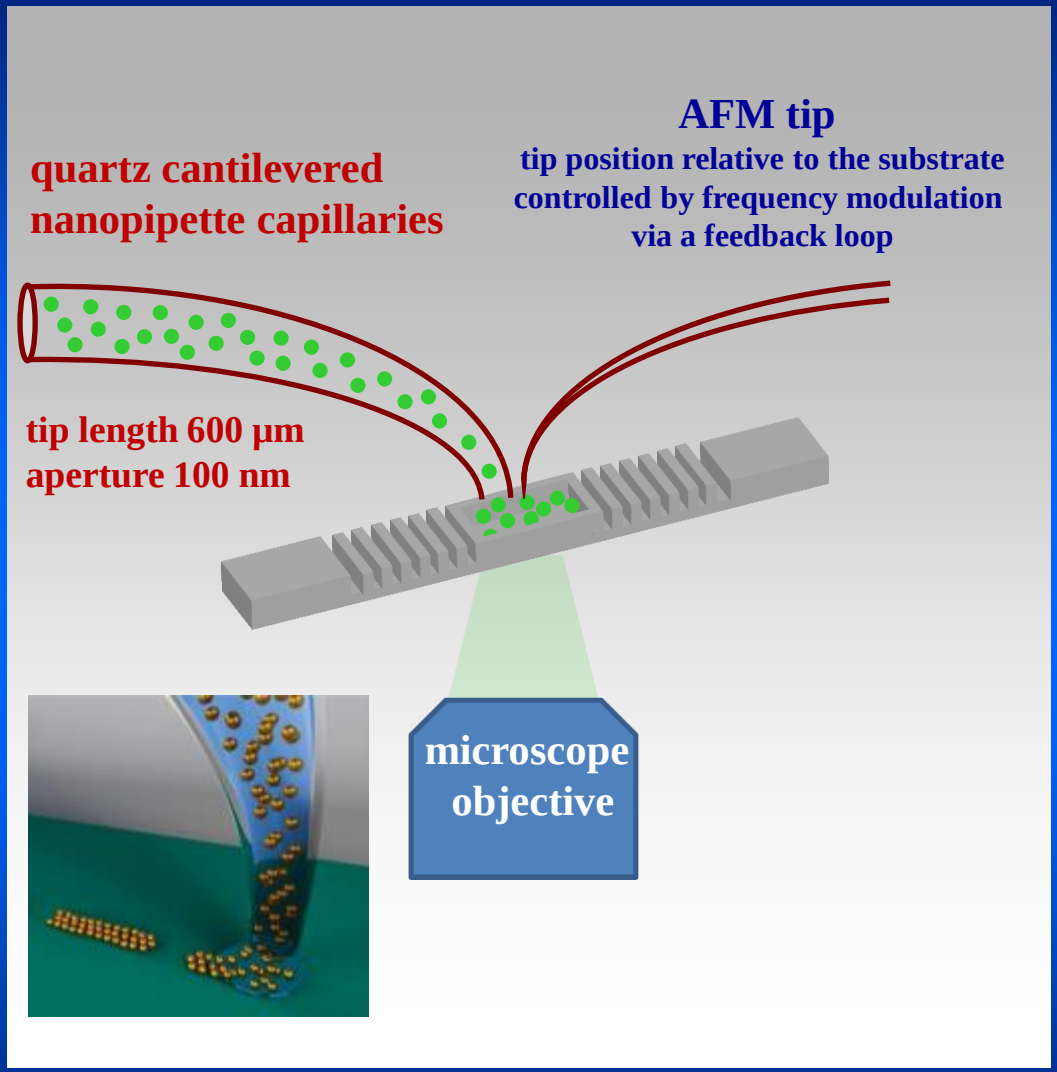


**Electrically-driven fountain pen nanolithography :**

**Scanning probe microscopy SPM + atomic force microscopy (AFM)**

# Transmission characteristics

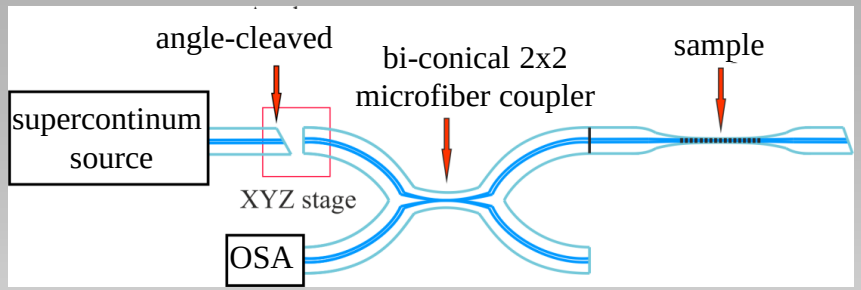


**Set-up for optical characterization of nanocavities**

- **microfibre coupler single mode operation bandwidth (400 nm-1700 nm)**
- **power splitting into the fundamental mode equally at the two output ports**
- **light reflected by the grating passed through the coupler and was recorded by an OSA**

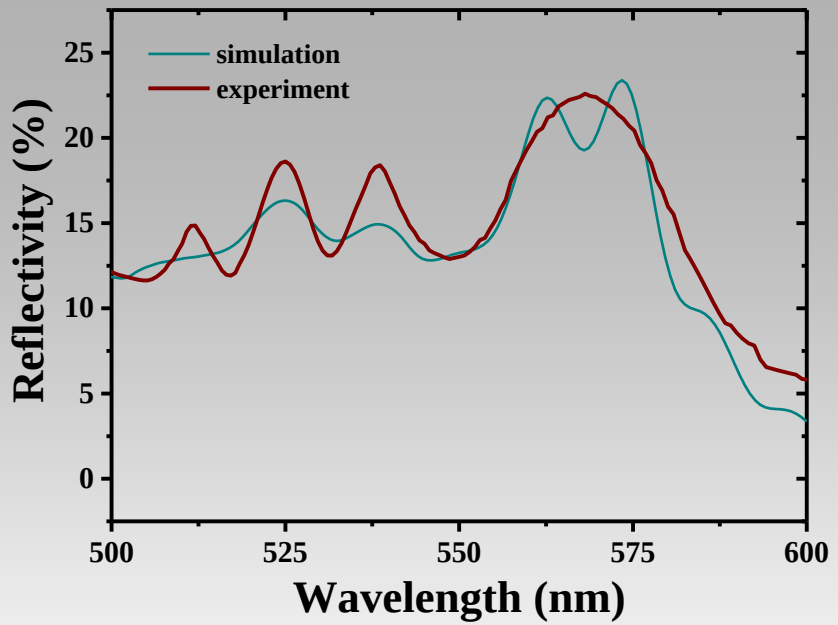


**Measured and simulated* reflectivity spectra of the nanocavity filled with the gain medium**

***Resonance wavelength : ~520 nm***

****finite-difference-time-domain (FDTD) method (Lumerical)***

# Electric field distributions

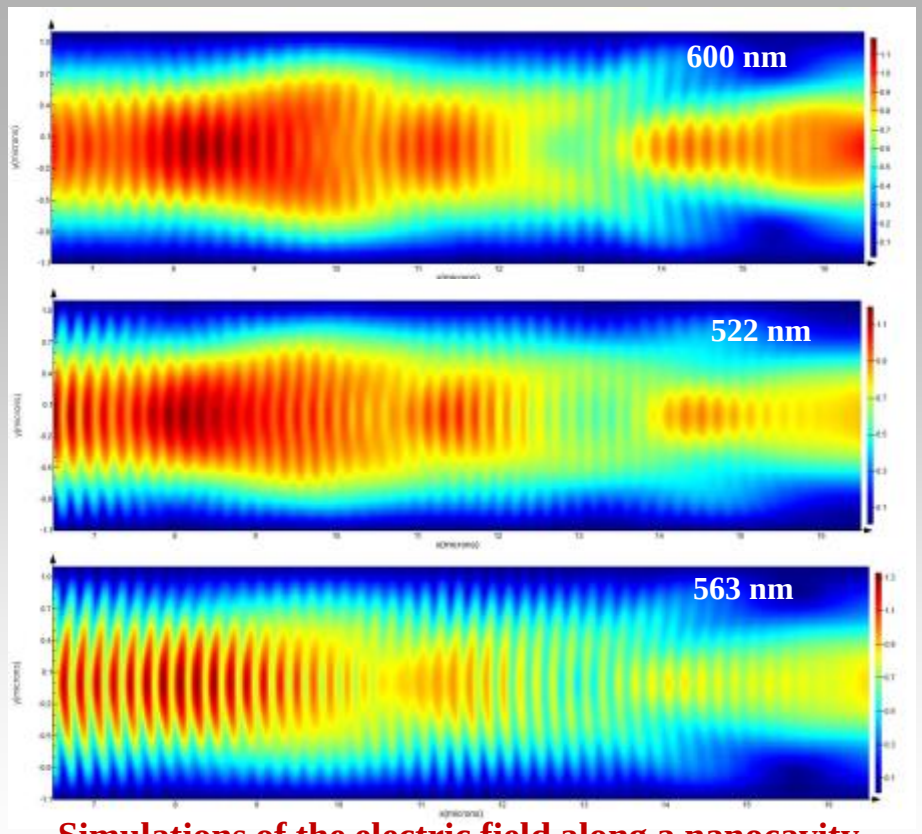


Simulations of the electric field along a nanocavity with 20 silica/air DBR gratings for 3 different wavelengths, propagating from left to right

## $CH_3NH_3PbBr3$ – filled nanocavities

- minimum reflectivity (600 nm): almost complete transmission through the waveguide
- energy confinement in the nanocavity for its resonance wavelength of 520 nm
- maximum reflectivity (563 nm): almost all the light is reflected

**Simulations field profiles for different wavelengths via the finite-difference-time-domain (FDTD) method (Lumerical)**

# Input-output characterics

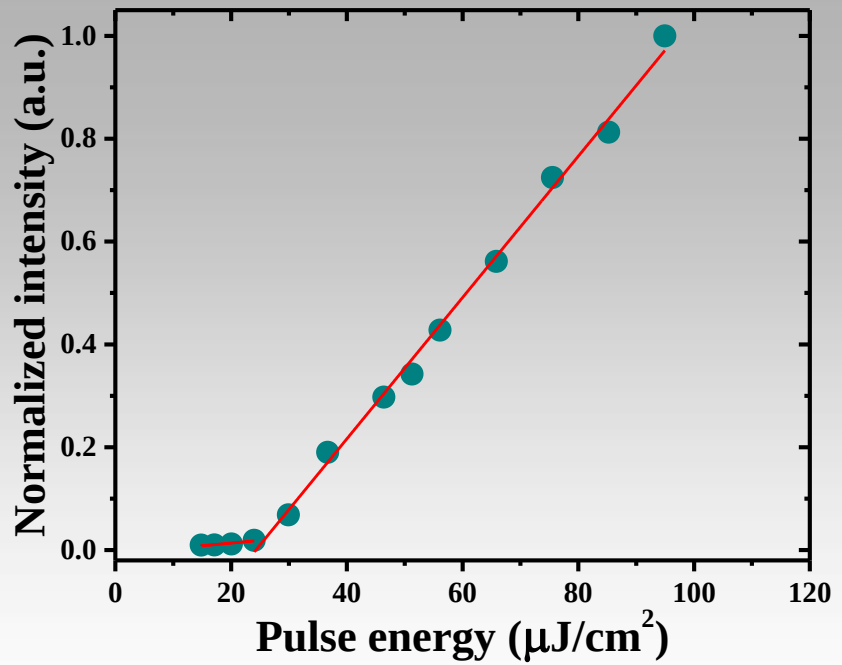


Laser output power as function of pump power for the single-mode laser operation

**Pump laser frequency-doubled Ti:sapphire amplifier:**

**λ=400 nm**

**repetition rate = 250 KHz**

**pulse width= 180-fs.**

- **Pump power threshold: 22 μJcm$^{-2}$**

# Tunability (experiment)

**Laser (3.5-μm, 200 fs, 80 MHz)**

**heating of the fiber**

**nanocavity with $P_{max}$= 80 mW**

**5 nm lasing wavelength tunability**

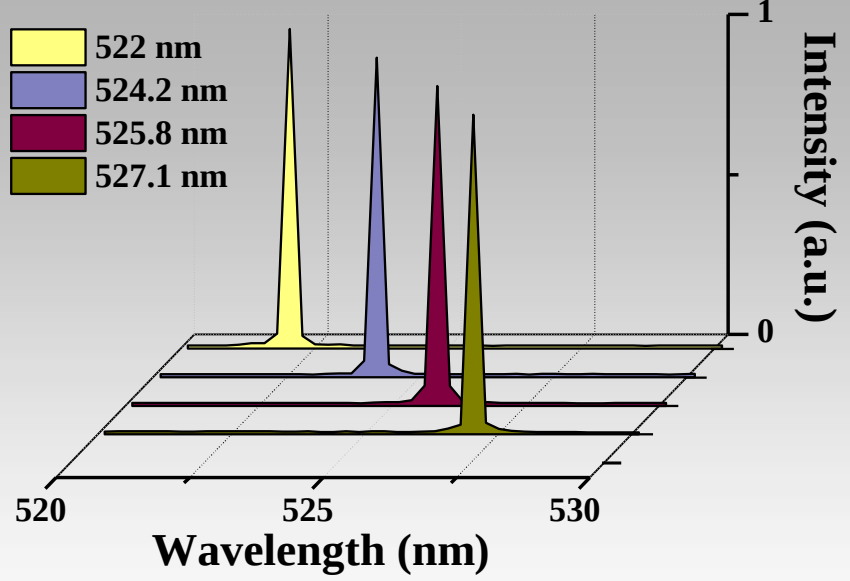


Laser emission lines obtained from the hybrid nanocavity for different output powers of the laser used for heating

- Heating laser power raised in successive steps and for each step the wavelength of the pump laser was modulated for resonant excitation
- Emission line gradually shifted in wavelength due to the increase in temperature
- The laser spectrum was recorded for each illumination power setting

# Tunability (calculations)

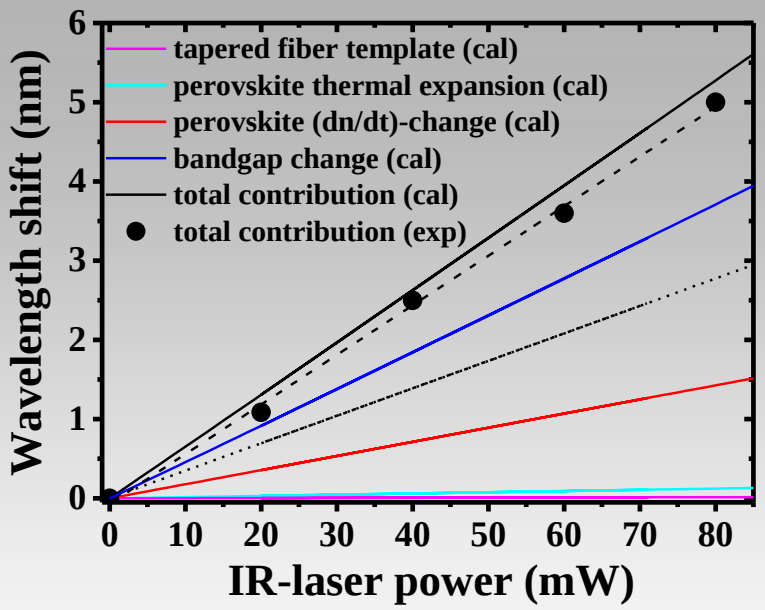


Calculated (black line) and measured (symbols) dependence of laser emission shift on heating laser power. The colored lines are calculations of the various contributions to the shift.

## Contributing Factors

- thermal expansion of the silica nanocavity
- thermal expansion of the perovskite nanocrystals
- thermo-optic effect in perovskites
- temperature-induced change of perovskite-bandgap

$$\Delta\lambda = \left( \alpha_s + \alpha_{nc} + \frac{dn_{nc}/dT}{n} \right) \Delta T + \Delta\lambda_{bg}$$

$\alpha_s$: thermal expansion coefficient (silica)

$\alpha_{nc}$: thermal expansion coefficient (perovskites)

$dn_{nc}/dt$: thermo-optic coefficient (perovskites)

$n_{nc}$=refractive index (perovskites)

$\Delta\lambda_{bg}$ : variation of bandgap wavelength

# Tunability (calculations)

**Analytical expression for maximum temperature of the hybrid nanocavity**

**Solution of the heat equation by adopting appropriate boundary conditions**

$$\Delta T = \left( \frac{P_{\max} \cdot P_{abs} \cdot \left(1 - R_{fr}\right) \cdot P_{gs}}{2 \cdot \sqrt{\pi} \cdot R_s \cdot \kappa_s} \right) \cdot \left( 1 + \frac{\kappa_a}{\kappa_s} \right)^{-1}$$

**$\Delta T \cong 39.6$ K**

$P_{max}$: maximum illumination power
$P_{abs}$ : % of $P_{max}$ absorbed by the silica
$R_{fr}$: Fresnel losses at the interfaces
$k_\alpha$: thermal conductivity of air

$P_{gs}$: coefficient for reflection losses due to the Gaussian laser profile and the curved surface of the sphere
$k_s$: thermal conductivity of silica

**$\Delta\lambda_{bg}$ can be calculated from the expression**

$$\Delta\lambda_{bg} = \left( \frac{-\lambda_g^2}{1239.6} \right) \cdot \Delta E_g \quad \text{where} \quad E_g(T) = E_g(0) - \left( \frac{\alpha \cdot T^2}{\beta + T} \right)$$

β :Debye temperature
α: temperature constant

**Experimental: $\Delta\lambda = 5.6$ nm**

**Calculation : $\Delta\lambda = 5.1$ nm**

**VERY GOOD AGREEMENT**

# Reduction of Auger recombination rates

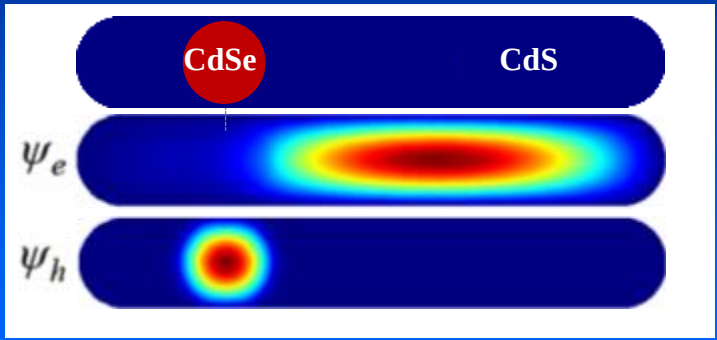


spatial distribution of wavefunctions,
to reduce electron-hole overlap and
and weaken exciton-exciton repulsion
C.Grivas et al. Nat. Commun. 4, 2376 (2013).

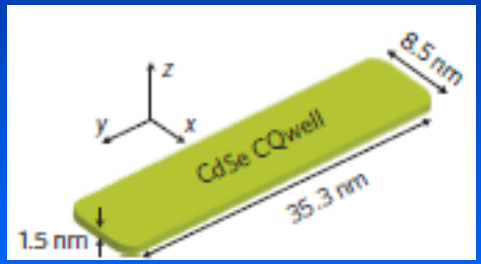


2D nanocrystal (quantum wells)
quantization of energy levels only in one direction,
thus a stricter momentum conservation rule
J. Grim et al. Nature Nanotech.
9, 891 (2014)

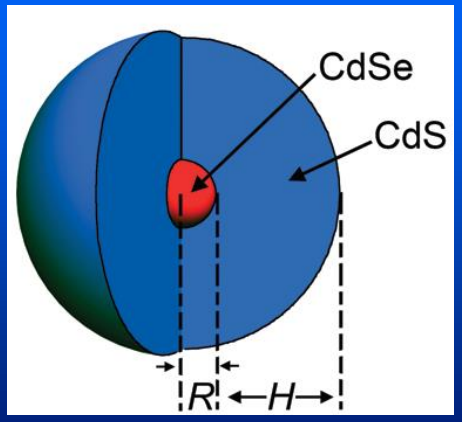


smoothing of the interfacial potential
via gradient alloy layer at the core/shell interface
F. Garcıa-Santamarıa et al. Nano Lett. 9, 3483
(2009), Dang et al. Nature Nanotech.7, 335–339 (2012)

# Quasi-cw lasing

2D perovskite nanocrystals → inherently slower Auger recombination rates
quantization of energy levels only in one direction,
thus a stricter momentum conservation rule

+

heat-sink → reduced thermally triggered Auger recombination rate

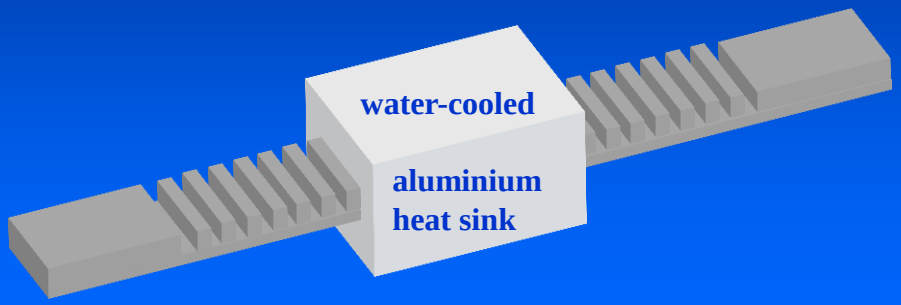


=

## Quasi continuous-wave lasing

Pump pulse duration : 300 ns

Duration of laser emission: ~1μs

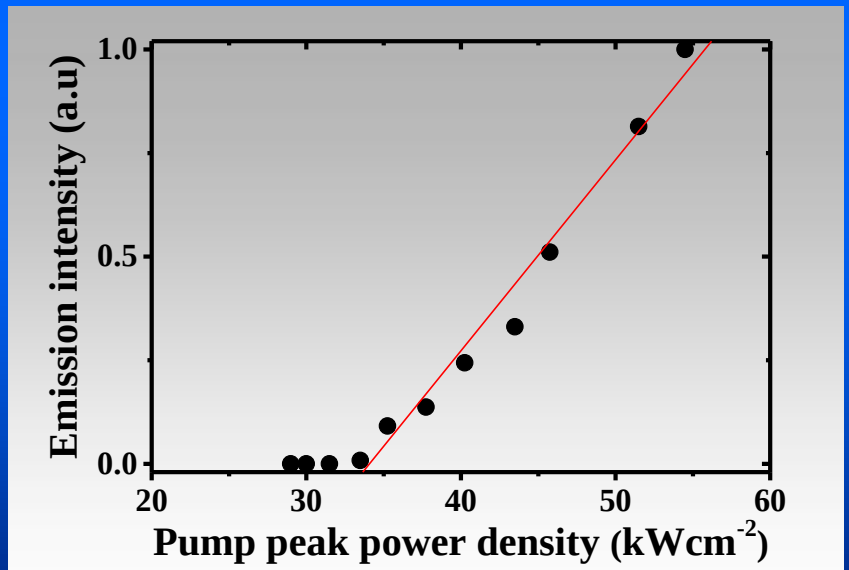


Input-output characteristics from 2D perovskite nanocrystals in a thermally managed nanocavity

# Conclusions

- Deposition of nanostructures in enclosed geometries via AFM-assisted nanolithography
- Tunable laser emission from hybrid perovskite nanodots in an optical fiber nanocavity
- Quasi-cw emission from all-inorganic 2D-perovskites nanocrystals with thermal management

# Outline

## Lasers based on semiconducting nanocrystals

**Gain media:** (i) Perovskite nanocrystals with various geometries such as platelets (single quantum wells) and nanowires
(ii) CdSe/CdS core/shell colloidal quantum rods

**Cavities:**

(i) Silica microspheres (ii) Diffractive cavities fabricated by (iii) Cavities formed by the gain m media themselves

(i.e nanowires)

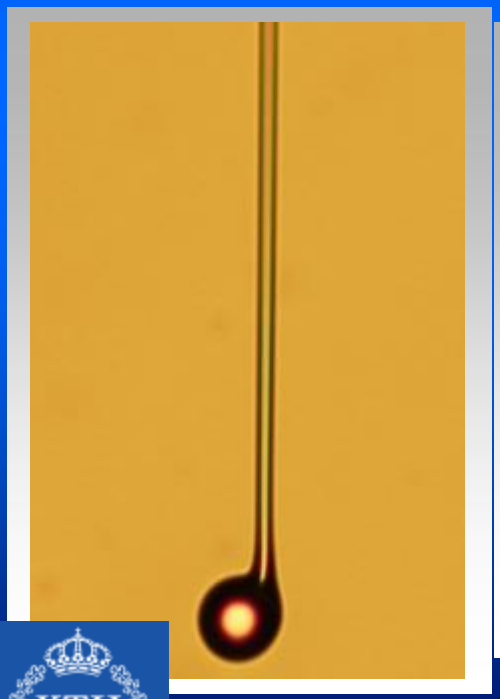

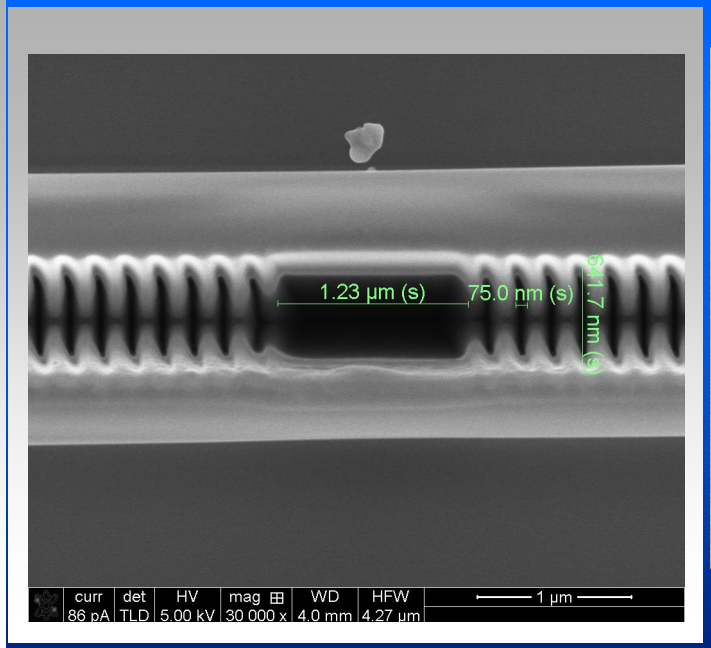


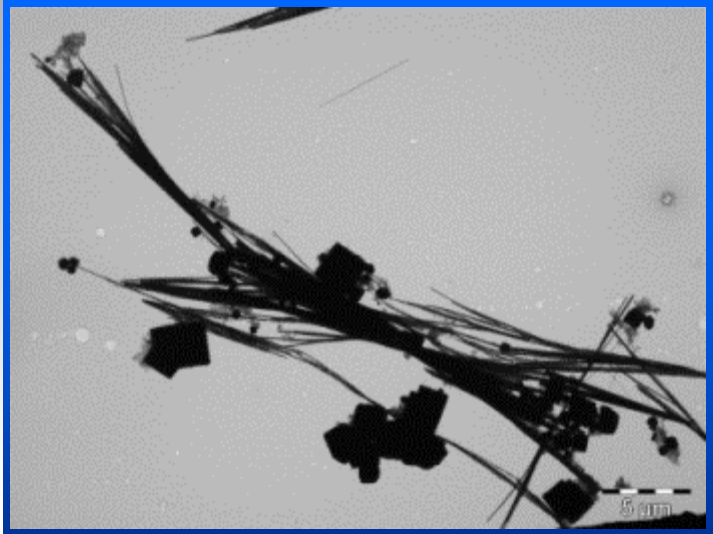



KTH VETENSKAP OCH KONST

UNIVERSITY OF Southampton

# Introduction

- Low cost synthesis based on wet chemistry

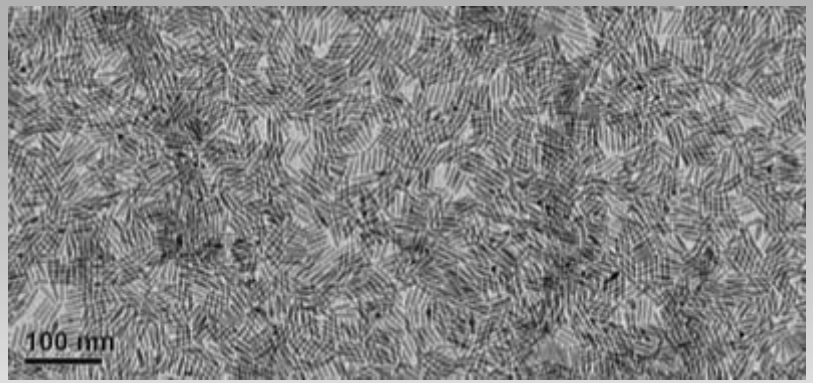


TEM image of colloid CdSe/CdS nanorods synthesized by the seeded-growth method

length = 27.734 ± 2.187 nm
diameter= 4.065 ± 0.624 nm

- Variability of physical shape and size
- Combination of material pairs for the core and shell

wavefunction engineering for the carriers within the nanorod and hence tuning the emission properties

# Introduction

- **Quasi-type II or type II ($0 \leq \Delta E \leq -0.3$ eV*) conduction band offset between CdSe and CdS**

* *C. Trager-Cowan et. Al. Semicond. Sci. Technol. (1992)*
*K. P. O'Donnell et al., J. Cryst. Growth (1992)*
*A. H. Nethercot et al., PRL (1974)*

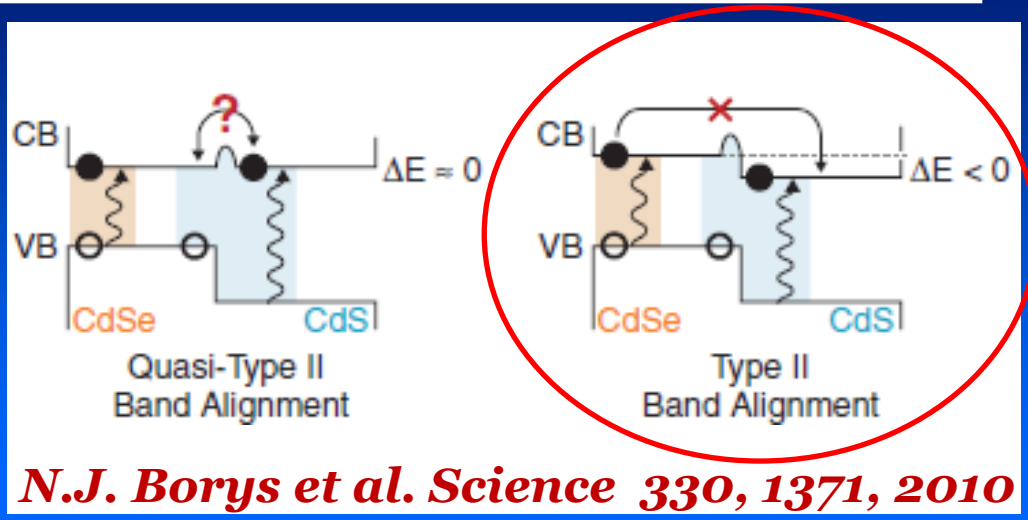


*N.J. Borys et al. Science 330, 1371, 2010*

## Type-II NQRs for single-exciton lasing

- Different spatial distributions of electron ($\psi_e$) and hole ($\psi_h$) wavefunctions
- Build up of large local charge densities and exciton-exciton repulsion
- Stark effect-related biexciton line shift with ect to the single-exciton ($\Delta_{XX} = E_{XX} - 2E_X$)

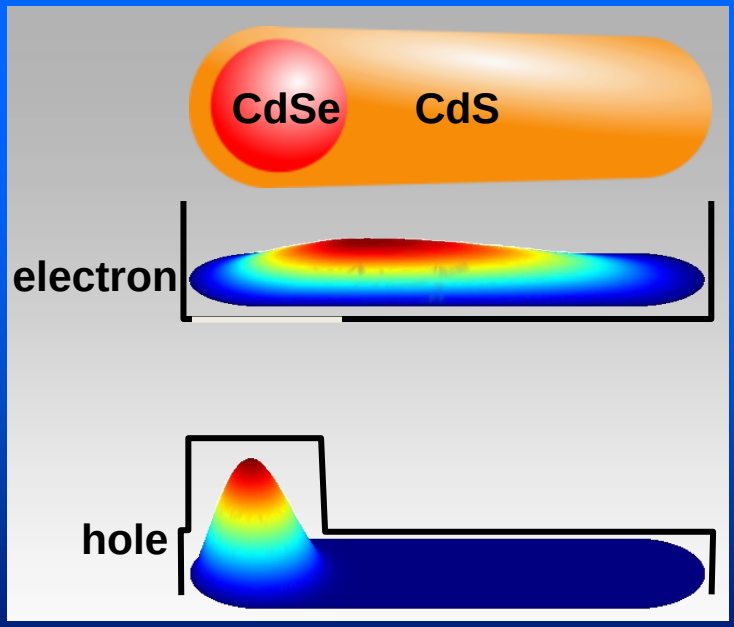

# Challenges

development of cost effective and simple of fabrication processes

development of nanoscale gain media

advanced integration into photonic integrated circuit (PIC) platforms/ nanointegration

miniaturization of the source layouts

development of sources using CMOS compatible materials

extension of the ranges of output characteristics (i.e. emission wavelengths pulse energies and repetition rates),

# Thank you for your attention!

# Fabrication Procedures

Microscope image of a silica microsphere template with a diameter of ~30 µm

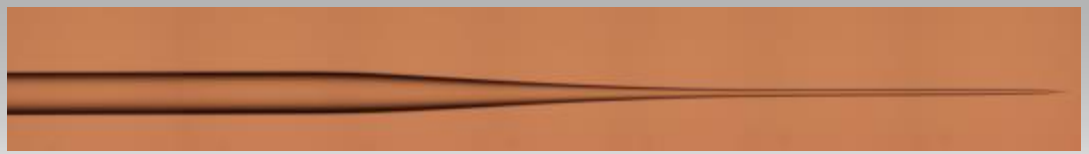

Microscope image of a fiber tip with diameter of 50 nm used to collect signals from the CdSe/CdS-nanocrystals /silica microsphere hybrid resonators

- **measured Q factors for uncoated silica microspheres: > $10^8$**
- **coating of the microspheres with a monolayer by dipping into a CdSe/CdS solution**

# Experimental set-up

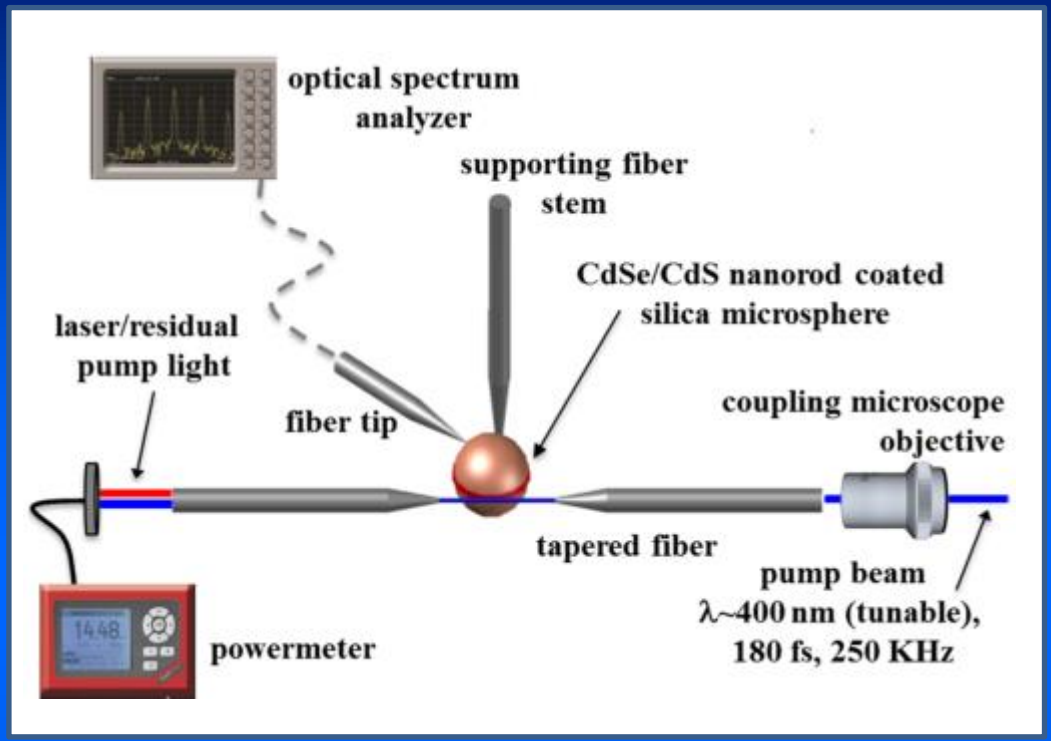


**Phase matching between the fundamental mode in the taper and a fundamental WGM**

- **Precludes pumping of higher radial mode index WGMs**
- **Enhanced pumping efficiency**

**Laser output readout:**

- **laser signal evanescently coupled into the taper**
- **unabsorbed pump removed with a suitable filter**

# Single-Mode Lasing

- ***resonant pumping*** **a fundamental WG pump mode with $|m| = l$ confined to the equatorial ring of the sphere and identified by a dip in the transmission through the taper when the pumping wavelength was tuned**

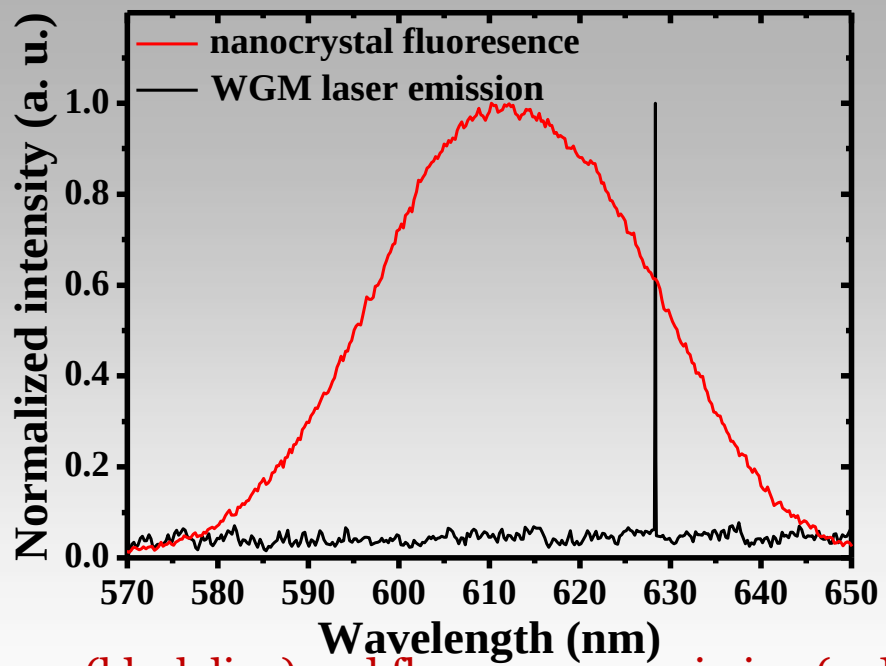


Laser (black line) and fluorescence emission (red line) from a 9.2-μm-diameter hybrid sphere and the nanorods on the sphere, respectively.

**Microspheres with sufficiently small size and FSR that is comparable to or larger than the bandwidth of the pump pulse, allows for spatially selective excitation of a single mode.**

- **FWHM of laser line : $\Delta\lambda$ = 0.06 nm**
- **The linewidth obtained suggests a value of Q ~$10^5$ for the coated microsphere**

# Open-access Fabry–Perot cavities (I)

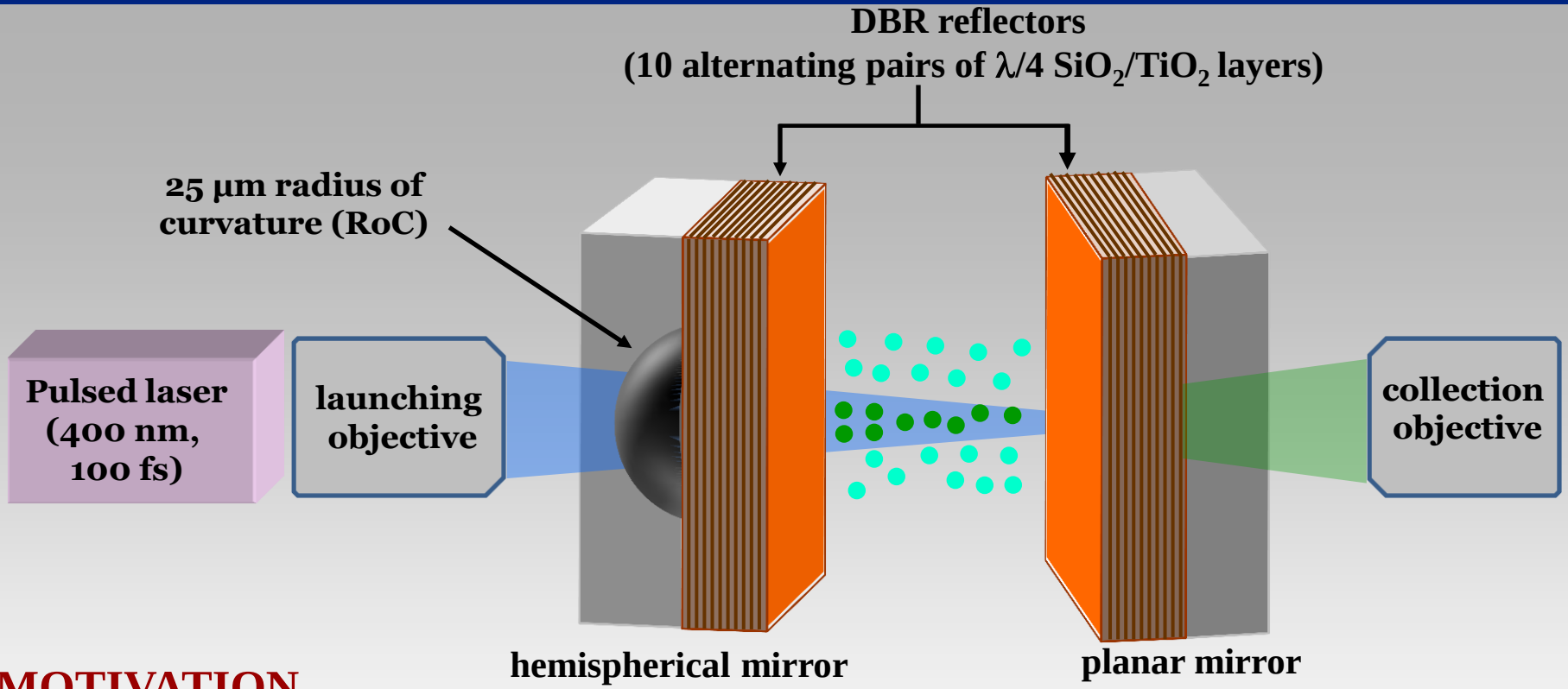


## MOTIVATION

- Open-access Fabry–Perot cavities with one planar and one concave mirror, enable formation of stable cavity modes confined in all three dimensions and formation of 0-dimensional polaritons (if $L < R_0C$). Interesting for investigating strong coupling effects in 2D materials

- Potential of platelets-shaped (single quantum well) perovskite (and other semiconductor nanocrystals for polaritonic lasers)

# Single-Exciton to Biexciton Lasing

## Non-equatorial pumping/pumping with high optical powers

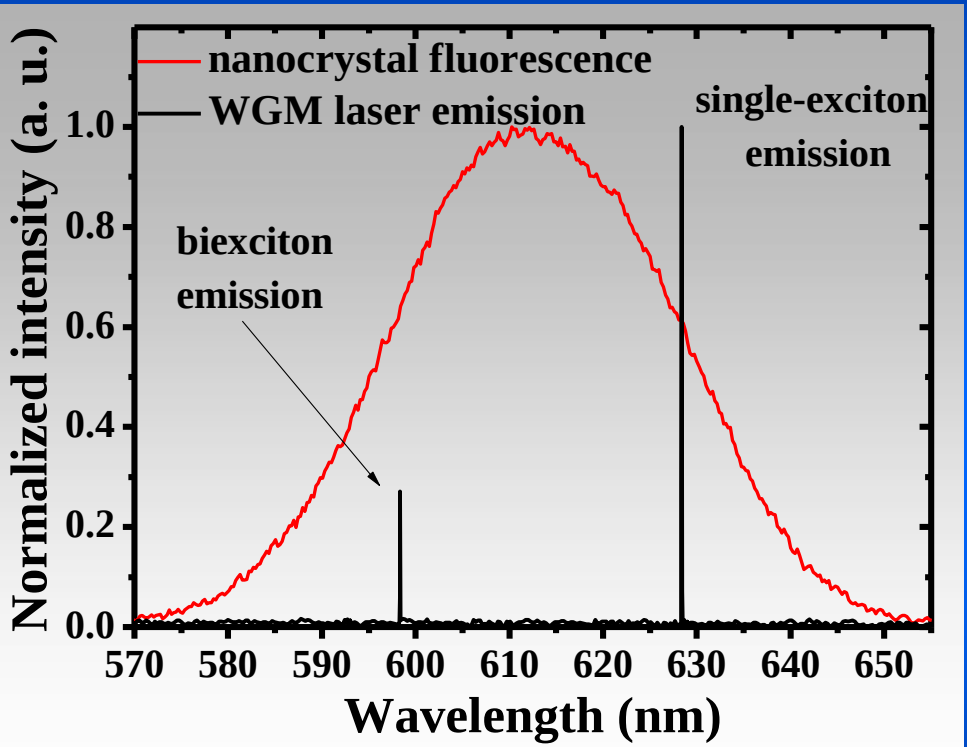


Laser emission obtained for 110 μW absorbed power by non-equatorial pumping

- **Lasing emission on both the single-exciton and the biexciton transitions**

# Multi-mode Lasing

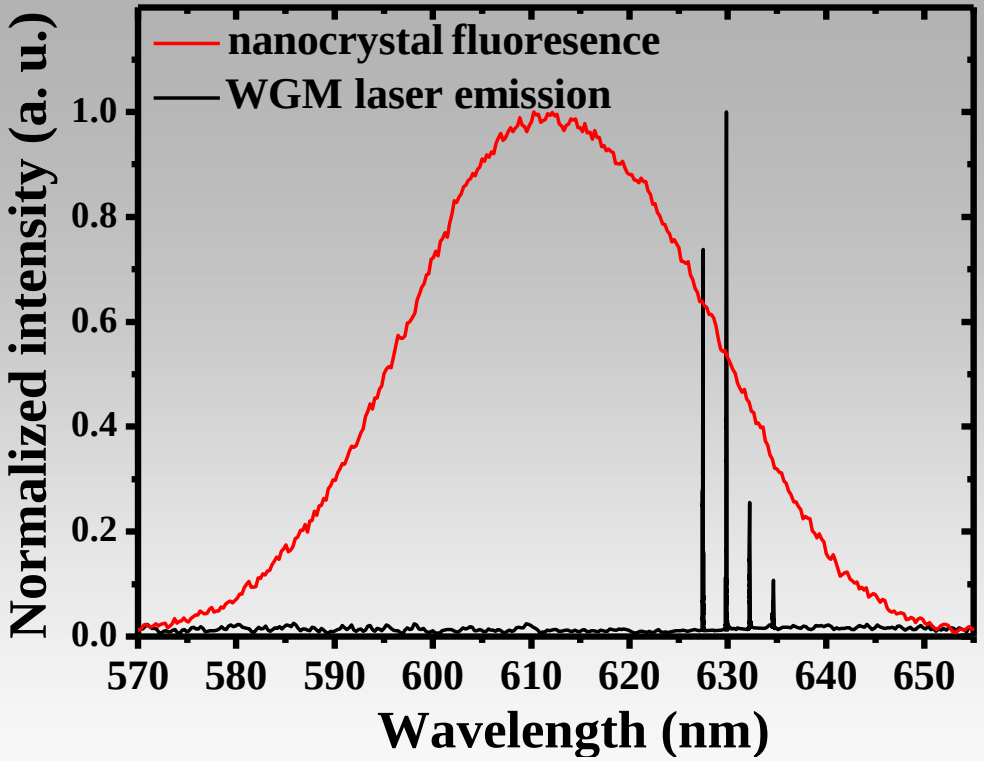


Multimode laser emission from a microsphere with a diameter of 29.4 mm. The equally spaced laser modes provide the FSR of the microsphere

**Lasing mode spacing (2.4 nm) in very good agreement with the free spectral range (FSR) of the microsphere ($\Delta\lambda_{FSR}$ = 2.375 nm) obtained from**

$$\Delta\lambda_{FSR}^{azim} = \left(\frac{\lambda_L^2}{2\cdot\pi\cdot R_H\cdot n_2}\right)\cdot\frac{\tan^{-1}\left[\left(n_1/n_2\right)^2-1\right]^{1/2}}{\left[\left(n_1/n_2\right)^2-1\right]^{1/2}}$$

$\lambda_L$ :emission wavelength ,

$n_1$ = 1.47 : refractive index of silica

$n_2$ = 2.5 : refractive index of the QNRs

$R_H$ : radius of the hybrid microsphere.

# Open-access Fabry–Perot cavities (II)

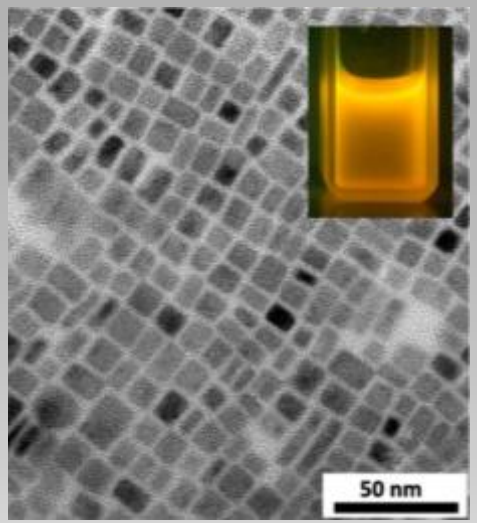


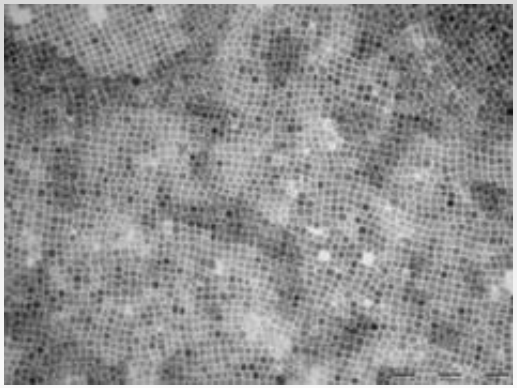

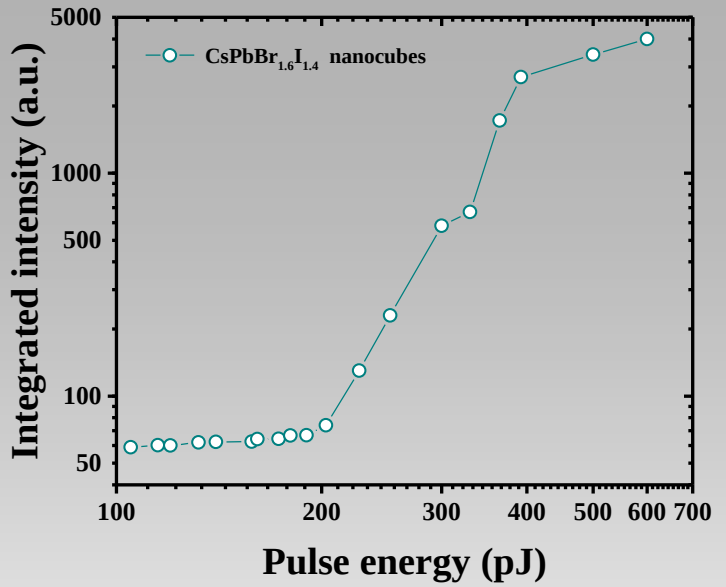


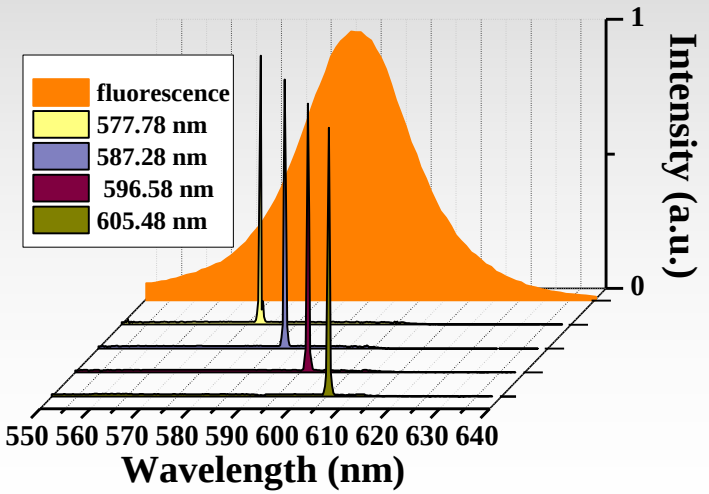


**$CsPbBr_{1.6}I_{1.4}$ nanocubes**

# Perovskite $CH_3NH_3PbBr_3$ nanowire laser

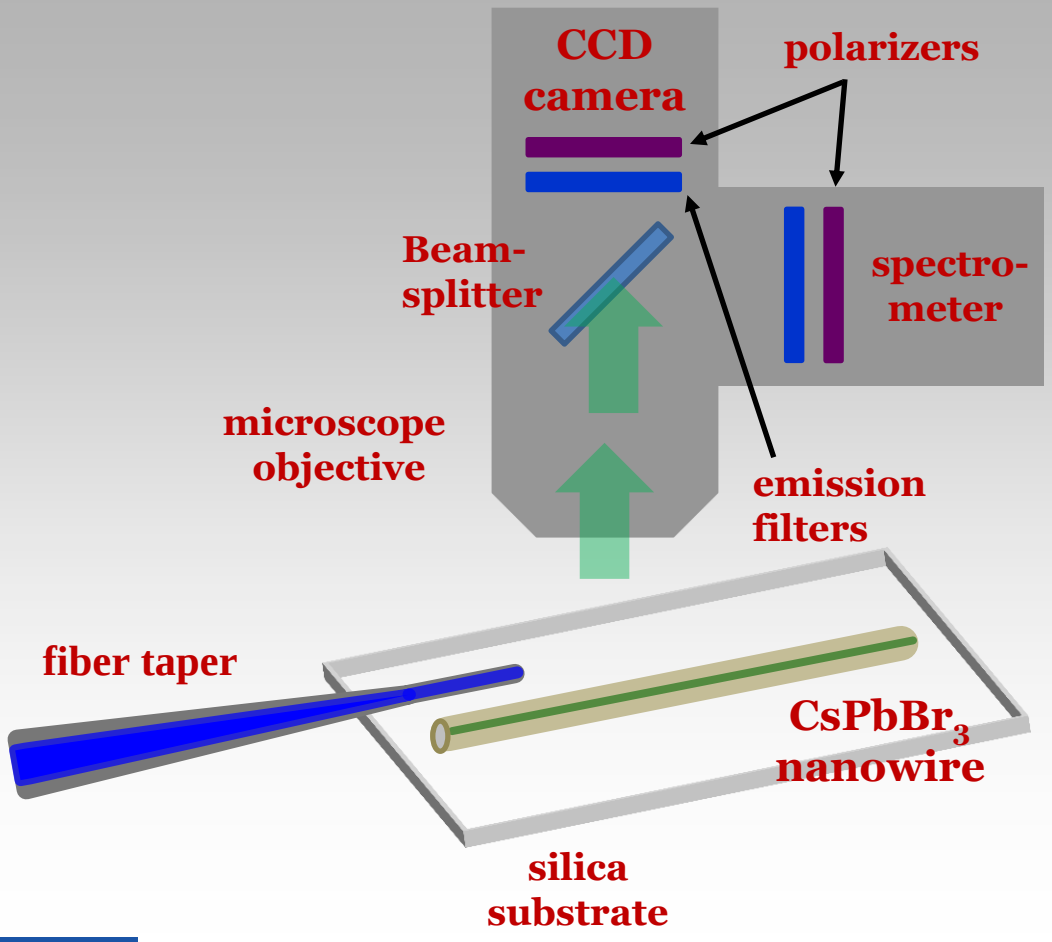


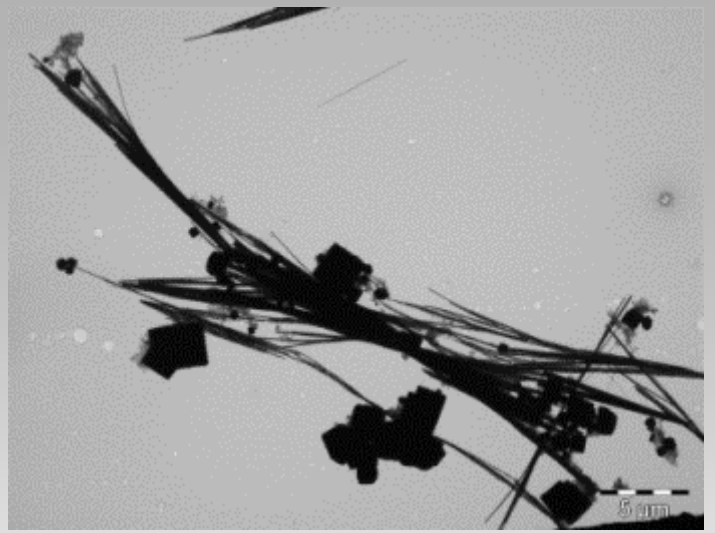


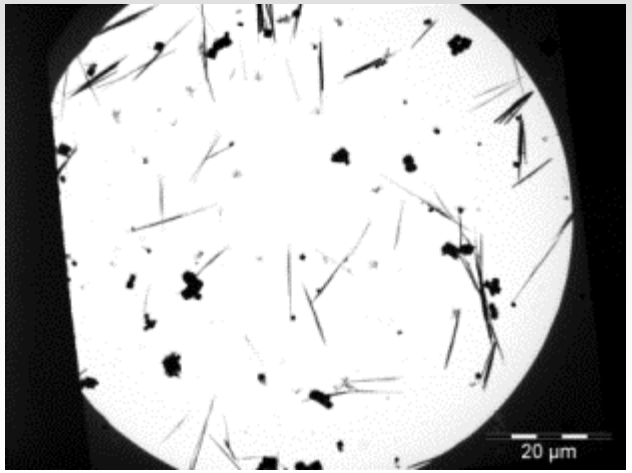

# Perovskite $CH_3NH_3PbBr_3$ nanowire laser